

(Read at the Autumn Meeting of The Society of Naval Architects of Japan, November, 1984)

# Self-Excited Vibration of Propeller Nozzles Experienced on Ocean-Going Tugboats

—1st Report—

by Yasunosuke Ogawa\*, *Member* Shinji Kumazaki\*, *Member*  
 Makoto Maeda\*, *Member* Katsuya Fujii\*\*, *Member*  
 Isao Neki\*, *Member* Masatetsu Shimono\*  
 Yasuhisa Okumoto\*, *Member*

## Summary

Despite every means available at the time of construction applied to prevent vibration, violent vibrations were reported on two ocean-going tugboats constructed by IHI, of size that places them among the world's largest. Measurements made of the vibration of aft part including nozzles and analysis of measured data revealed that the vibrations of nozzles:-

- were constant in frequency, irrespective of propeller or engine revolution, and attained values of acceleration reaching 8,000 Gal;
- were generated only under certain conditions of operation, and diminished to very low levels under all other conditions;
- corresponded to what is known as flow-induced vibration, and were closely associated with the water flow around the nozzles.

Two possibly ascribable mechanisms were considered as cause of the self-excited vibration.

- (1) Locked-in vibration induced by Karman's vortex street;
- (2) Occurrence of negative damping (known as "galloping").

Neither of these two mechanisms have so far proved conclusively assignable as cause: (1) Karman's vortex streets on account of uncertainty in estimating the exciting force under lock-in condition, and (2) galloping for lack of definite tendency of the negative slope of nozzle lift vs. attack angle curve.

The vibrations observed being of such amplitude as to permit no delay in remedial action, measures were taken to counteract both the mechanisms considered above: (1) Karman's vortex streets by attaching fins to the nozzles to decrease their trailing edge thickness, and hence to modify the shedding frequency of the vortex streets, and avoid resonance; (2) galloping by strutting the two nozzles together so as to constrain them to in-phase vibration mode, which was considered from observation of the damping behavior to be conducive to marked modification of the structural and mass damping performance, and consequently convert the damping to positive value.

Vibration measurements reperformed after applying the above measures proved the violent vibrations to have been completely eliminated, evidencing ample effectiveness of the measures adopted. Further token of the effectiveness of the measures is provided by the complete absence of reports from either tugboat on violent vibrations, throughout the two years that have since elapsed, during which the tugboats have each marked over 4,000 hours of active service.

\* Shipbuilding & Offshore, Ishikawajima-Harima Heavy Industries Co., Ltd.

\*\* Yokohama Research Institute, Ishikawajima-Harima Heavy Industries Co., Ltd.

## 1. Introduction

Two ocean-going tugboats—of capacity that places them amongst the world's largest—were completed by IHI in October and December 1979. At the time of their construction, every means

currently available was applied to prevent vibration<sup>1)</sup>, but nevertheless, after their delivery, the crew of both tugboats reported violent vibrations experienced in the accommodation space and the aft part where the propellers and nozzles were equipped. In January 1982, an extensive series of vibration measurements was carried out jointly between IHI and the Owners of the tugboats. The measurements were made with underwater accelerometers mounted on the nozzles and surrounding parts.

It was established as a result that the vibrations occurring on the nozzles and around stern.

- were constant in frequency, irrespective of propeller or engine revolution, and attained values of vibration acceleration reaching 8,000 Gal,
- were generated only under certain conditions of operation, and diminished to very low levels under all other conditions,
- corresponded to what is known as flow-induced vibration, and were closely associated with the water flow around the nozzle.

The foregoing factors were indicative of a phenomenon that was hardly foreseeable from the state of knowledge of ship vibrations at the time of construction of the tugboats.

Based on the information thus assembled, together with the data that had been recorded at the time of construction, measures for eliminating the violent vibrations were planned, and were applied to the tugboats in April and September 1982. Vibration measurements were then remade, to verify the effectiveness of the measures thus applied.

Two years have elapsed since then, and the tugboats have each already marked over 4,000 hours of active service, but no reports have since been received of violent vibrations experienced in either tugboat.

In this paper, the characteristics of the violent vibrations are noted, their probable causes are discussed, the measures successfully applied are indicated, and the effectiveness of the measures are verified.

## 2. Principal Particulars of the Tugboats

The rough arrangement of the tugboats is shown in Fig. 1; Table 1 presents the principal particulars. Notable characteristics are: Twin-engine, twin-screw, controllable-pitch propellers rotating in fixed nozzles; 20,800 SHP engine output, 200 tf towing force, 19.4 kt service speed.

As shown in Fig. 2, the 4 m diameter nozzle is connected above through head box to the stern, and below to the lower end of the shaft bracket by means of strut. This arrangement of nozzle support was adopted on considerations detailed in

Table 1 Principal particulars

Lbp	90.0 m
Molded breadth	15.8 m
Molded depth	8.0 m
Molded draft	6.0 m
Main engine	IHI-S.E.M.T.-Pielstick diesel engine 16PC2-5V X 2 sets
Maximum output of main engine	10,400 PS X 520 rpm X 2 sets
Propeller	4-blade controllable pitch propeller (with fixed nozzle) X 2 sets
Revolutions (main engine/propeller)	340-520/110-168rpm
Speed	19.4 kt
Maximum towing force	200 tf
Classification	NK, NS* (Tug/Salvage)

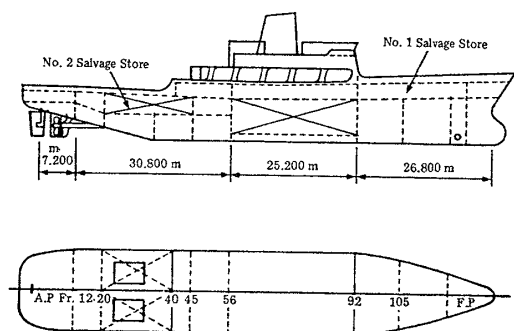


Fig. 1 Rough arrangement

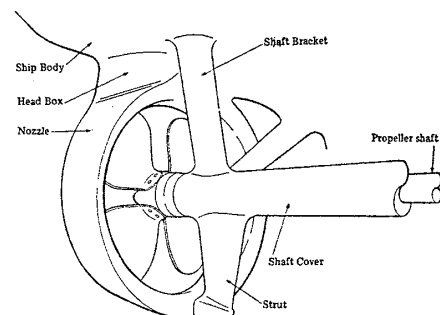


Fig. 2 Plan of nozzle

Reference<sup>1)</sup>.

## 3. Vibration Measurements

### 3.1 Arrangement for measurements

While the tugboats were docked, underwater accelerometers were mounted on the nozzles and surrounding parts protected by watertight sealing, as indicated in Fig. 3, and vibration measurements were made after undocking.

The conditions at measurement are presented in Table 2. Runs 1 and 3 were made with tugboat running free, of which Run 1 was made under normal conditions of auto-program control, in which tugboat speed was controlled by propeller

Table 2 Ship's condition

NO.	1	2	3	4
ITEM	PROGRESSIVE SHAFT R.P.M. MEASUREMENT	PRELIMINARY TOWING MEASUREMENT	PROGRESSIVE BLADE PITCH MEASUREMENT	TOWING MEASUREMENT
DATE	16 <sup>TH</sup> JAN '82	24 <sup>TH</sup> JAN '82	24 <sup>TH</sup> JAN '82	28 <sup>TH</sup> JAN '82
PLACE	OFF EJIMA	OSAKA BAY	OSAKA BAY	OSAKA BAY
WEATHER	FINE	FINE	FINE	CLOUDY
SEA CONDITION	CALM	CALM	CALM	SLIGHT
DEPTH OF WATER	DEEPER THAN 20 m	DEEPER THAN 16 m	DEEPER THAN 16 m	DEEPER THAN 16 m
DISPLACEMENT	abt 4,700 t	abt 4,800 t	abt 4,800 t	abt 4,900 t
df	5.3 m	5.3 m	5.3 m	5.3 m
da	5.5 m	5.7 m	5.7 m	5.8 m
dm	5.4 m	5.5 m	5.5 m	5.55 m
PROPELLER IMMERSION	120 %	125 %	125 %	128 %
NOZZLE IMMERSION	107 %	111 %	111 %	113 %
TOWING FORCE	0 t	max. 45 t	0 t	max. 153 t

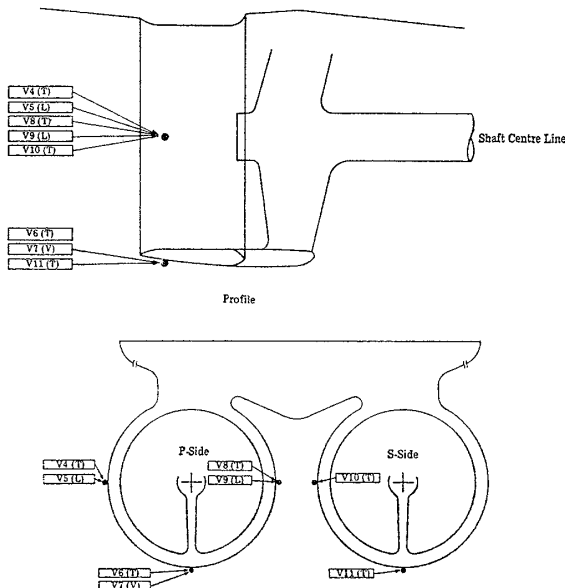


Fig. 3 Arrangement of measuring points

blade pitch at 110 rpm propeller revolution, and above this revolution, controlled by propeller revolution with blade pitch fixed at about 32°. Run 3 was made with propeller revolution held constant and with tugboat speed controlled by propeller blade pitch. Runs 2 and 4 were made while maximum towing loads of 45 and 153 tf, respectively.

The measured revolutions and propeller pitch angles are indicated in Fig. 4.

3.2 Results of measurement

3.2.1 Run 1 (auto-program control)

Measurements were made with propeller revolution varied from 110 to 163 rpm in steps of 3 rpm. The strongest vibration was recognized at the measuring point V6, the frequencies composing the vibration at this point being as represented by the spectrum of Fig. 5. The accelera-

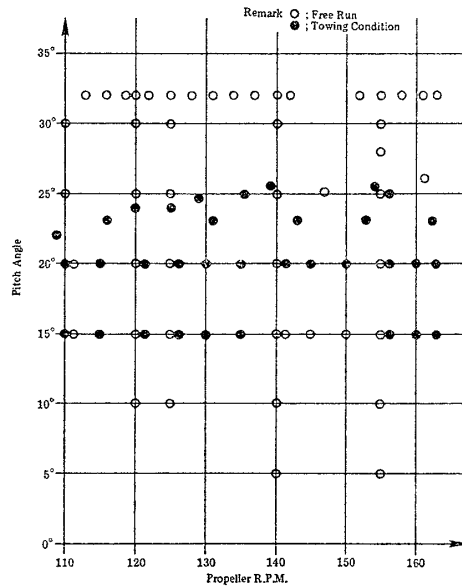


Fig. 4 Measuring pitch angle and propeller RPM

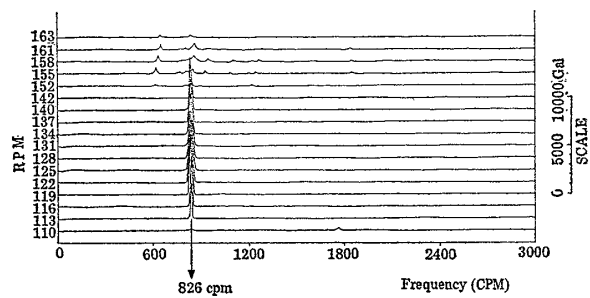


Fig. 5 Spectrum analysis V6(T)

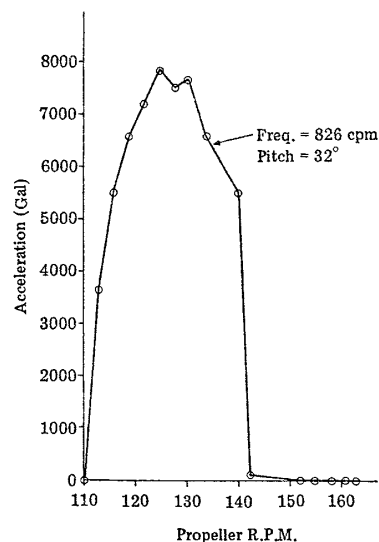


Fig. 6 Vibration acceleration V6(T)

tion level at 826 cpm for each propeller revolutions is shown in Fig. 6; Fig. 7 represents the vibration mode measured at 125 rpm, at which the highest acceleration was recognized. During these

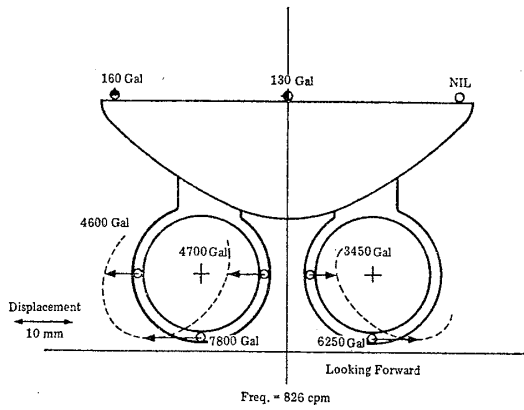


Fig. 7 Vibration mode (125 RPM) pitch = 32°

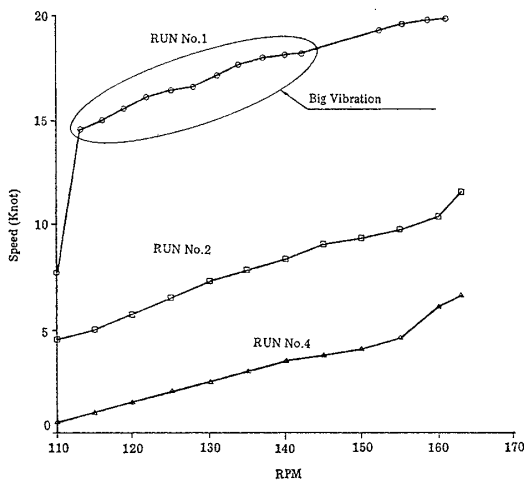


Fig. 8 Ship's speed at vibration measurements

measurements, the tugboat speed changed as shown in Fig. 8.

The foregoing data indicate that:

- (1) Vibration was prominent in the range of revolutions from 113 to 140 rpm; outside this range, the vibrations diminished markedly.
- (2) The violent vibration was generated uniquely at the constant frequency of 826 cpm.
- (3) The nozzles vibrated laterally in anti-phase mode; vibration was slightly higher level on the port side nozzle.
- (4) The violent vibration was generated at 14 to 18 kt tug speed.

### 3.2.2 Run 3 (pitch control)

This run was made to examine the relation between propeller blade pitch and vibration. The accelerometer readings from the measuring point V6 at 125 and 140 rpm are reproduced in Fig. 9, where the time scale is reduced for clarity.

It is seen that vibration is negligible when the propeller blade pitch is below 30°, beyond which

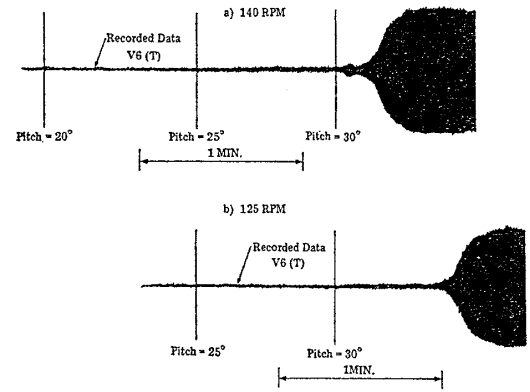


Fig. 9 Effect of pitch

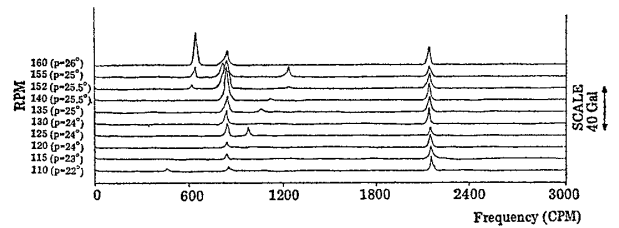


Fig. 10 Spectrum analysis V6(T) (towing condition)

it increases sharply.

### 3.2.3 Runs 2 and 4 (towing condition)

An example of vibration analysis is presented in Fig. 10, which reveals that when towing, the violent vibrations observed when running free were no longer generated, the highest acceleration recorded being only 32 Gal at measuring point V6 in both Runs.

## 4. Discussion on Cause of Vibration

A discussion is presented on the probable mechanism that generates the extraordinary vibrations noted in the preceding Section 3.2.

### 4.1 Measured vibration magnitude

Fig. 11 presents the relation between propeller RPM and frequencies of the measured data given in Fig. 5.

It is revealed that the violent vibrations correspond to none of the frequencies that would normally be considered to affect the stern part of hull—i.e. multiples of propeller shaft revolution (1, 4=Number of blades, 8=Twice number of blades, ...)—and that the frequency is constant and irrespective of propeller revolution. This frequency of 826 cpm is, as shown in Fig. 12, close to the natural frequency of 800 cpm measured with vibration exciter applied to hull stern while moored<sup>1)</sup>, and the present value can be considered to represent the corresponding natural frequency while running.

The above behavior of the inordinate vibra-

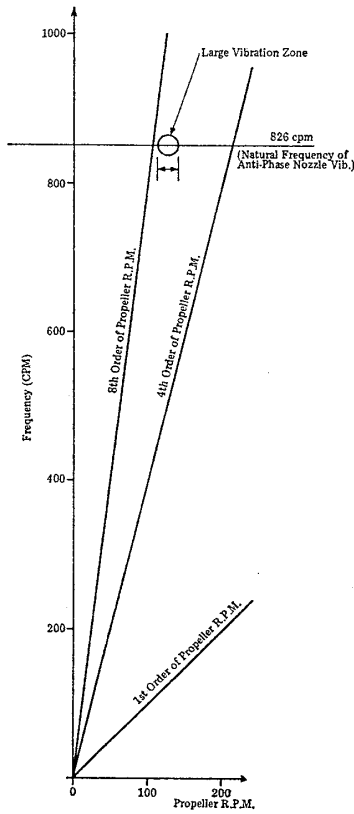


Fig. 11 Relation between propeller RPM and frequencies

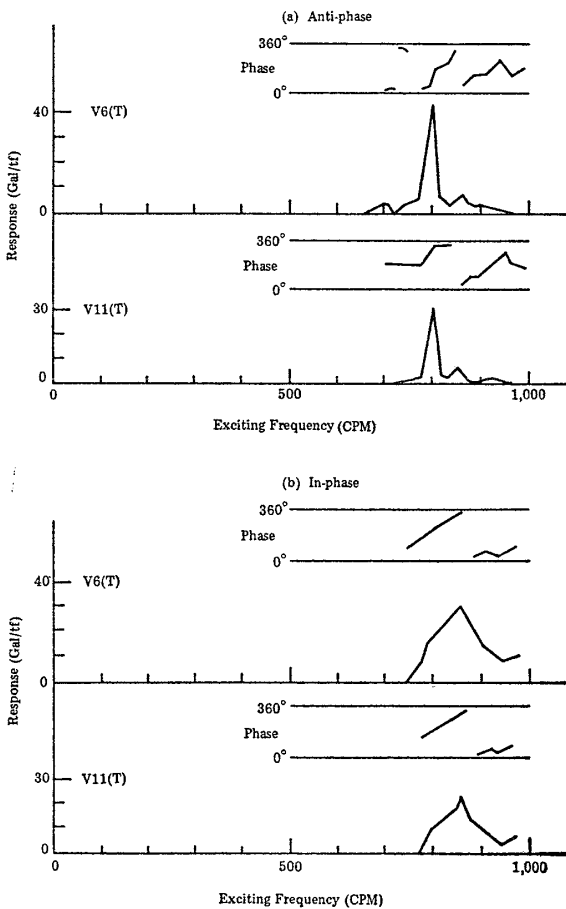


Fig. 12 Results of exciter test

tions is characteristic of what is known as self-excited vibration.

4.2 Self-excited vibration

Upon examining the various factors that govern the self-excited vibration affecting the nozzles, the probable causes were narrowed down to:

- (1) Locked-in vibration caused by Karman's vortex street
- (2) Self-excited vibration generated on account of the nozzle damping characteristics becoming negative—i.e. phenomenon known as "galloping".

4.2.1 Karman's vortex street

We first examined the likelihood of the cause of violent vibrations being Karman's vortex street, which is rarely experienced in practice.

The exciting frequency should in such case be

$$f = 60 \cdot U_0 \cdot c / d, \quad (\text{cpm}) \quad (4.1)$$

where

- $U_0$ : Flow velocity (m/s)
- $d$ : Nozzle trailing edge thickness (=0.1 m)
- $c$ : Strouhal coefficient (=0.15-0.20)

Substituting into Eq. (4.1) the tugboat speed derived in Section 3.2.1 (4), the estimated exciting frequency

$$f = 648 - 1,110 \text{ cpm},$$

is obtained.

The frequency of 826 cpm obtained from actual measurement is situated in the mid range of this exciting frequency. This suggests the violent vibrations in question to be assignable to what is known as forced self-excited vibration by Karman's vortex street with the vortex-shedding frequency in the above range locked-in to the 826 cpm of nozzle natural frequency.

The exciting force can be estimated practically [as follows<sup>2)</sup>,

$$w = 1/2 \cdot \rho U_0^2 d C_L Q, \quad (4.2)$$

where

- $w$ : Exciting force per unit length of nozzle (kgf/m)
- $\rho$ : Specific gravity of fluid (=104.6 kgf·s<sup>2</sup>/m<sup>4</sup>)
- $C_L$ : Lift coefficient for round bar<sup>2)</sup> (=0.15)
- $Q$ : Magnification factor (=80).

Therefore, in the flow velocity range of 14 to 18 kt which corresponds to the violent vibrations,

$$w = 3255 - 5382 \text{ kgf/m}.$$

If the vortex street exciting force is considered to have been generated in the part indicated in Fig. 13, the total exciting force

$$F = w \cdot \pi \cdot D \cdot 120 / 360 \text{ kgf},$$

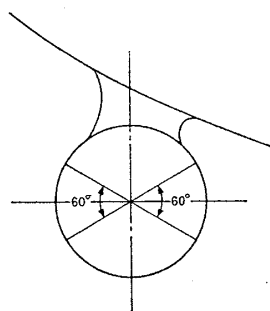


Fig. 13 Assumed range of Karman's vortex street

where

$D$ : Nozzle diameter (=4 m).

Therefore,

$$F = 13,635 - 22,544 \text{ kgf.}$$

The spring constant of the nozzle structure is calculated as 180 tf/mm, as derived from its transverse rigidity which had been determined at the time of initial design. Hence, the amplitude of vibration that would be excited by the Karman's vortex street would be

$$\begin{aligned} \delta &= F/180,000 \\ &= 0.076 - 0.125 \text{ mm,} \end{aligned}$$

which is 2 orders of magnitude smaller than the measured value of around 10 mm and this is one element of doubt on the cause by Karman's vortex street. Another element of doubt is whether the vortex street would actually exert a force conducive to lateral vibration of the nozzles, when continuity of the vortices is considered.

On the other hand, it has been found<sup>3)</sup> that once Karman's vortex street would be locked-in, the value of  $C_L$  in Eq. (4.2) can depart widely from that of forced vibration, and the results, the vibration amplitude can be extraordinary increased.

The effect of this lock-in would not permit Karman's vortex street to be immediately dismissed as possible cause of the violent vibrations.

#### 4.2.2 Self-excitation by negative damping

##### (1) Mechanism

A freely damping system of 1 degree of freedom will be governed by the equation of motion

$$\ddot{y} + 2\epsilon\dot{y} + \nu^2 y = 0, \tag{4.3}$$

which represents a periodic motion when  $\epsilon < \nu$ , and a general solution can be obtained as

$$y = A e^{-\epsilon t} \cdot \cos(\sqrt{\nu^2 - \epsilon^2} \cdot t + B), \tag{4.4}$$

where, letting the period  $T = 2\pi / \sqrt{\nu^2 - \epsilon^2}$ , the ratio of amplitudes between the instants  $t_0$  and  $t_0 + T$  should become

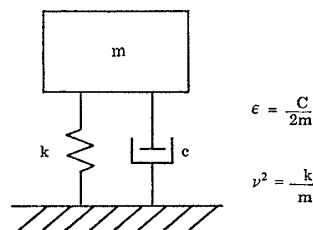


Fig. 14 Model of free vibration

$$|y_{t=t_0+T}| / |y_{t=t_0}| = e^{-\epsilon T}, \tag{4.5}$$

which indicates a vibration attenuating with each cycle if  $\epsilon > 0$ , whereas when  $\epsilon < 0$  an amplifying vibration that strengthens with each cycle is indicated.

The latter case represents the mechanism of self-excitation generated by negative damping.

##### (2) Application to the present instance

The nozzle placed in fluid stream, modeled for simplicity to represent one degree of freedom, is illustrated in Fig. 15, in which diagram,

$$F_L = 1/2 \rho U_R^2 D^2 C_L \tag{4.6}$$

$$F_D = 1/2 \rho U_R^2 D^2 C_D, \tag{4.7}$$

where

- $F_L$ : Lift for one nozzle king (kg)
- $F_D$ : Drag for one nozzle ring (kg)
- $U_R$ : Resultant velocity (m/s)
- $C_L$ : Lift coefficient of one nozzle ring
- $C_D$ : Drag coefficient of one nozzle ring

We here assume that:

- $\dot{x} = 0, U_x = U_0;$
- $U_y = 0, |\dot{y}| \ll U_0, \alpha = -\dot{y}/U_0;$
- $U_R^2 = U_0^2 + \dot{y}^2.$

Now, the resultant force in the  $y$ -direction

$$\begin{aligned} F_y &= F_L \cos \alpha + F_D \sin \alpha \\ &= 1/2 \rho U_R^2 D^2 (C_L \cos \alpha + C_D \sin \alpha). \end{aligned} \tag{4.8}$$

Hence, the equation of motion governing the model of Fig. 15 becomes

$$(m + m_{add}) \ddot{y} + C \dot{y} + k y = F_y, \tag{4.9}$$

where

$m_{add}$ : Added water mass.

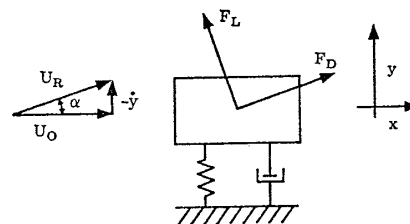


Fig. 15 Model of nozzle in flow

By letting

$$F_y = 1/2 \rho U_0^2 D^2 C_y, \quad (4.10)$$

and substituting this  $F_y$  into Eq. (4.8), we have

$$C_y = (C_L \cos \alpha + C_D \sin \alpha) (U_R/U_0)^2. \quad (4.11)$$

On the other hand, since  $\alpha$  is very small,

$$\left. \begin{aligned} C_L(\alpha) &= C_L(0) + \left(\frac{\partial C_L}{\partial \alpha}\right)_{\alpha=0} \cdot \alpha + 0(\alpha^2) \\ C_D(\alpha) &= C_D(0) + \left(\frac{\partial C_D}{\partial \alpha}\right)_{\alpha=0} \cdot \alpha + 0(\alpha^2) \\ \cos \alpha &= 1 - 0(\alpha^2) \\ \sin \alpha &= \alpha \\ (U_R/U_0)^2 &= 1 + 0(\alpha^2) \end{aligned} \right\} \quad (4.12)$$

By substituting Eq. (4.12) into Eq. (4.11),

$$C_y = C_L(0) - \left\{ \left(\frac{\partial C_L}{\partial \alpha}\right)_{\alpha=0} + C_D(0) \right\} (\dot{y}/U_0). \quad (4.13)$$

In this equation,  $C_L(0)$  is a static load, so that the dynamic component

$$C_y = - \left\{ \left(\frac{\partial C_L}{\partial \alpha}\right)_{\alpha=0} + C_D(0) \right\} (\dot{y}/U_0). \quad (4.14)$$

By substituting Eqs. (4.14), (4.10) into Eq. (4.9), we derive the equation of motion

$$\left[ (m + m_{add}) \ddot{y} + \left\{ C + (1/2) \rho U_0 D^2 \left\{ \left(\frac{\partial C_L}{\partial \alpha}\right)_{\alpha=0} + C_D(0) \right\} \right\} \dot{y} + k \right] \ddot{y} = 0, \quad (4.15)$$

where

$C$ : Structural and mass damping

$$1/2 \rho U_0 D^2 \left\{ \left(\frac{\partial C_L}{\partial \alpha}\right)_{\alpha=0} + C_D(0) \right\} :$$

Dynamic damping .

In order for Eq. (4.15) to constitute the self-excitation referred to in Item (1), the coefficient of the 2nd term of Eq. (4.15) must have a nega-

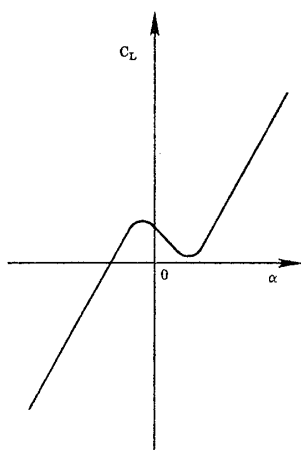


Fig. 16 An example of  $\alpha$ - $C_L$  curve

tive value. Now, generally,  $C$  and  $C_D(0)$  are positive, so that a necessary condition for the above requirement would be  $(\partial C_L/\partial \alpha)_{\alpha=0} < 0$ . Thus, violent vibration could be induced in the case indicated in Fig. 16, where, for flow attack on the nozzle at angle  $\alpha=0$ , the nozzle lift shows a negative slope. The present nozzle can be considered to present such a case.

(3) Measured negative damping

We derive in what follows the actual negative value of  $\epsilon$  in Eq. (4.3) from the measured data at the violent vibration given in Fig. 9.

It was found that the difference of vibration amplitude was quite small for  $\Delta t=T$ , and so  $\epsilon$  was derived for  $\Delta t=10T$ :

From Eq. (4.5) with  $T$  replaced by  $10T$ , we have

$$\epsilon = -(1/10T) \ln (|y_{t=t_0+10T}|/|y_{t=t_0}|). \quad (4.16)$$

Substituting into Eq. (4.16)

$$T = 2\pi/\nu_d, \quad \zeta = \epsilon/\nu_d,$$

where

$$\nu_d = \sqrt{\nu^2 - \epsilon^2},$$

we have the damping ratio

$$\zeta = -(1/20\pi) \ln (a_n + 10/a_n). \quad (4.17)$$

where

$a_n$ : Double amplitude of data at  $n$ -th cycle

The actual values of  $a_n$  corresponding to the measured data are presented in Table 3, from which a negative damping ratio was obtained as

$$\zeta = -0.0026.$$

This means that the violent vibrations are based on the assumption of negative damping adopted in Sections 4.2.2. (1) and (2), though the

Table 3 Calculation of negative damping

n	$a_n$	$\delta^*$	n	$a_n$	$\delta^*$
0	6	0.00800	240	95	0.00622
10	6.5	0.02683	250	101.1	0.00520
20	8.5	0.01112	260	106.5	0.00223
30	9.5	0.02336	270	108.9	0.00528
40	12	0.00408	280	114.8	0.00384
50	12.5	-0.008338	290	119.3	0.00394
60	11.5	0.01226	300	124.1	0.00379
70	13	0.00377	310	128.9	0.00177
80	13.5	0.01054	320	131.2	0.00204
90	15	0.00953	330	133.9	0.00445
100	16.5	0.02647	340	140	0.00420
110	21.5	0.01706	350	146	0.00449
120	25.5	0.01790	360	152.7	0.00227
130	30.5	0.02458	370	156.2	0.00272
140	39	0.01138	380	160.5	0.00136
150	43.7	0.01347	390	162.7	0.00067
160	50	0.01467	400	163.8	0.00229
170	57.9	0.00796	410	167.6	-0.00108
180	62.7	0.00738	420	165.8	-0.00018
190	67.5	0.00548	430	165.5	0.00102
200	71.3	0.00893	440	167.2	-0.00072
210	78	0.00965	450	166	-0.00042
220	85.9	0.00455	460	165.3	
230	89.9	0.00552			

$\delta^* = \frac{1}{10} \ln \left( \frac{a_n + 10}{a_n} \right)$      $a_n$ : Double Amp. of Data at  $n$ -th cycle  
 mean = 0.01618  
 $\therefore \zeta = -0.0026$

nozzle lift characteristics of negative slope have not been verified.

### 5. Measures Adopted for Preventing Violent Vibration

The acceleration affecting the nozzles in question being of quite prominent intensity, as indicated from the data shown in Figs. 5, 6 and 7, it was felt that delay in implementing measures for abating the vibration risked serious damage. For this reason, measures to this end were immediately applied against both the causes considered probable in the preceding Chapter 4, while the studies for further pinpointing the true cause were continued in parallel.

#### 5.1 For eliminating vibration due to Karman's vortex street

Fins were mounted on the trailing edge of the nozzles, so as to decrease the trailing edge thickness from 100 mm to 16 mm, hence to modify the vortex shedding frequency of the Karman's vortex streets, and thereby to avoid the resonance.

#### 5.2 For eliminating self-excited vibration due to negative damping

The measure devised to eliminate vibration due to the mechanism discussed in Section 4.2.2 was as described below.

We simplify the expression of Eq. (4.15) by representing its 2nd term in the form

$$\zeta_T = \zeta_{ST} + \zeta_{SEV}, \quad (5.1)$$

where

$\zeta_T$ : Total damping ratio of nozzle

$\zeta_{ST}$ : Structural mass damping ratio of nozzle

$\zeta_{SEV}$ : Hydrodynamic damping ratio

We have seen in Section 4.2.2. (3) that

$$\zeta_T = -0.0026.$$

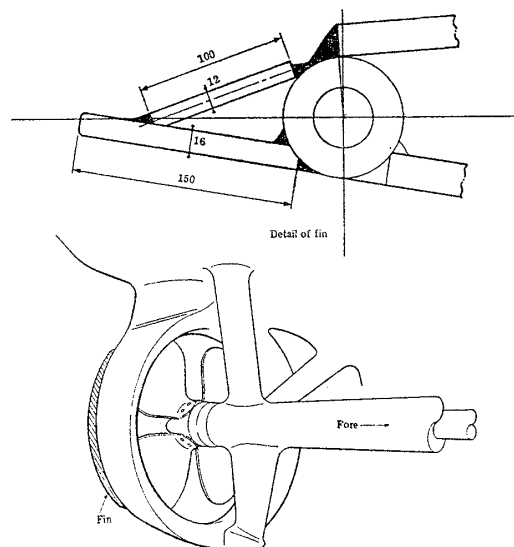


Fig. 17 Rough sketch of new fin

Self-excited vibration should be suppressible by rendering this value of  $\zeta_T$  positive.

The results of external excitation applied to hull stern while moored<sup>1)</sup> (Fig. 12) indicated that there was a marked difference in peak shape between the anti-phase and in-phase modes of vibration, which strongly suggested a large difference in damping ratio between the two modes of vibration. The actual values of structural and mass damping ratio estimated from measured data by Half Power Point method are.

$$\zeta_{ST} = 0.0056 \text{ for anti-phase vibration mode of nozzle} \quad (5.2)$$

$$\zeta_{ST} = 0.0326 \text{ for in-phase vibration mode of same,} \quad (5.3)$$

thus proving the damping ratio to be 6 times larger for the in-phase in comparison with anti-phase mode.

Substituting into Eq. (5.1) the value for  $\zeta_{ST}$  given by Eq. (5.2) and

$$\zeta_T = -0.0026,$$

we have

$$\zeta_{SEV} = -0.0082 \quad (5.4)$$

for anti-phase vibration mode of the nozzles. Assuming this hydrodynamic damping to remain unchanged and using  $\zeta_{ST}$  in Eq. (5.3), we can calculate the total damping for in-phase mode as

$$\begin{aligned} \zeta_T &= 0.0326 - 0.0082 \\ &= 0.0244 (>0). \end{aligned} \quad (5.5)$$

This is resulting in a positive value of damping ratio, which should serve in eliminating the self-excited vibration.

Thus, the in-phase mode of vibration was imposed on the nozzles by strutting them to each other in the arrangement illustrated in Fig. 18.

#### 5.3 Effectiveness of the measures

After applying the measures vibration measurements were reperformed, again using underwater accelerometers, in order to verify the effectiveness of these measures. The measurements

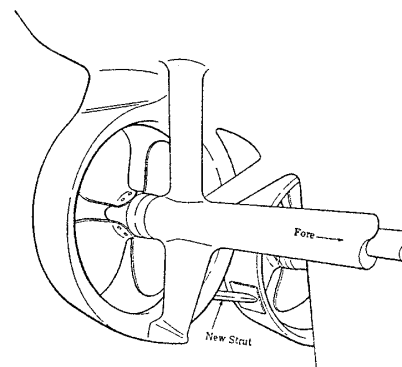


Fig. 18 Rough sketch of new strut

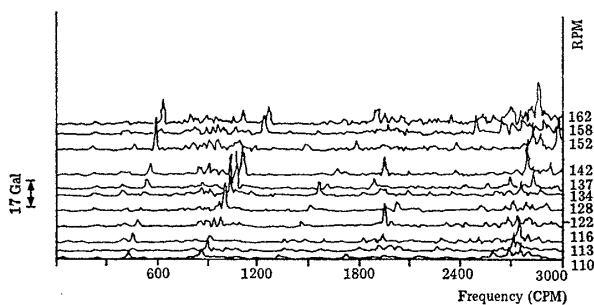


Fig. 19 An example of spectrum analysis V6(T) after measures were adopted

were conducted 4 times—twice on each tugboat—which revealed complete suppression of all violent vibration such as observed in the previous Runs 1 and 3.

As an example of the measured data, Fig. 19 reproduces the spectrum analysis of data from the measuring point V6, which had recorded the largest acceleration.

It is thus revealed that the self-excited vibrations that had affected the nozzles have been completely suppressed by the measures described in Section 5.5.

## 6. Concluding Summary

Two twin-engine twin-screw tugs built by IHI ranking amongst the world's largest—20,800 SHP, 200 tf towing force, 19.4 kt service speed—and equipped with controllable-pitch propellers and fixed nozzles, were found after entrance into service to be affected by violent vibration of the nozzles.

The vibrations were measured and analyzed, from which it proved that:

- (1) The vibrations occurred only in the range of propeller revolution between 113 and 140 rpm, and when the propeller blade pitch was at an angle exceeding  $30^\circ$ .
- (2) The vibration frequency was invariably 826 cpm irrespective of propeller and engine revolution.

These facts pointed toward self-excited vibration induced by interaction between water flow and hull structure as cause of the violent vibrations, a phenomenon that had hardly ever been considered previously in ship vibration studies.

The two probable mechanisms considered as cause of this self-excited vibration were:

- (1) Locked-in vibration induced by Karman's vortex streets occurring downstream of the nozzle trailing edges.
- (2) Occurrence of negative damping.

Examination has so far proved neither of these probable mechanisms to be conclusively assignable as cause of the violent vibrations: (a)

Karman's vortex street was found upon calculation to provide excitation amplitude 2 orders of magnitude smaller than actually observed; the other surmise (b) of negative damping remains to be substantiated by definite tendency of the nozzle lift characteristic presenting a negative slope against attack angle  $\alpha$  around  $0^\circ$ .

Nonetheless, the vibrations observed were of such amplitude as to permit no time to be lost in investigations before taking remedial measures. For this reason, action was taken to counteract both the mechanisms considered probable: (a) Karman's vortex street by attaching fins to nozzle to modify the resonance velocity, and hence the exciting frequency, and (b) negative damping, by strutting between the two nozzles to modify the damping to positive value.

Vibration measurements reperformed after applying the above measures proved the violent vibrations to have been completely suppressed, evidencing ample effectiveness of the measures adopted.

Thus, while the immediate practical need of eliminating the violent vibrations affecting tugboat service operation has been satisfactorily solved, studies have been continued to investigate the true cause of the self-excited vibrations, as well as the pattern of flow past nozzle that induces the vibration. Other questions remaining to be answered include defining the range of operating conditions (propeller loading etc.) that should leave the nozzles free from vibration, and the elements of nozzle design that should contribute to avoiding vibration excitation. The results will be reported on the 2nd Report.

In closing, the authors express their deep appreciation of the unreserved cooperation in according every facility for vibration measurements provided by the Owners of the two tugboats. Grateful acknowledgment is also due to Dr. Tadashi Matsudaira, now retired former IHI Research Institute Director, and Dr. Masaharu Kunieda, IHI Technical Advisor for their valuable advice and encouragement throughout the course of the present study.

## Reference

- 1) Okumoto, Y., Yamazaki, K., Kumazaki, S.: Vibration of Ocean Tugboat IHI Engineering Review Vol. 14 No. 1 (Jan. 1981).
- 2) Japan Road Association: Specifications for highway bridges (Feb. 1981).
- 3) Dr. Naudascher, E.: Flow-induced forces and vibrations Text book of Intensive Lectures on Flow-induced Vibrations, Tokyo, Japan (Sept. 1982).